Journal of Fluids and Structures ▮ (▮▮▮▮) ▮▮▮–▮▮▮

Contents lists available at ScienceDirect

Journal of Fluids and Structures

journal homepage: www.elsevier.com/locate/jfs

Flow over a cylinder subjected to combined translational and rotational oscillations

Mehdi Nazarinia [a], David Lo Jacono [c,b,a], Mark C. Thompson [a], John Sheridan [a,*]

[a] Fluids Laboratory for Aeronautical and Industrial Research (FLAIR), Department of Mechanical and Aerospace Engineering, Monash University, P.O. Box 31, Melbourne, Victoria 3800, Australia

[b] Université de Toulouse; INPT, UPS; IMFT (Institut de Mécanique des Fluides de Toulouse); Allée Camille Soula, F-31400, Toulouse, France

[c] CNRS; IMFT; F-31400 Toulouse, France

ARTICLE INFO

Article history:
Received 17 November 2010
Received in revised form
18 May 2011
Accepted 20 May 2011

Keywords:
Vortex shedding
Combined oscillation
Lock-on
PIV

ABSTRACT

The experimental research reported here employs particle image velocimetry to extend the study of Nazarinia et al. (2009a), recording detailed vorticity fields in the near-wake of a circular cylinder undergoing combined translational and rotational oscillatory motions. The focus of the present study is to examine the effect of the ratio between the cross-stream translational and rotational velocities and frequencies on the synchronization of the near-wake structures for multiple phase differences between the two motions. The frequencies are fixed close to that of the natural frequency of vortex shedding. The results are presented for a fixed amplitude of rotational oscillation of 1 rad and a range of ratios between the translational and rotational velocities (V_R) = [0.25,0.5,1.0,1.5] and for a range of frequency ratios (F_R) = [0.5,1.0,2.0]. In particular, it was found that varying the V_R value changed the near-wake structure. The results show that at the lower value of $V_R = 0.25$, for all of the phase differences examined, the vortices are shed in a single-row 2*S* mode aligned in the medial plane with a slight offset from the centreline and also synchronized with the combined oscillatory motion. As V_R increases the vortex shedding mode changes from a 2*S* single-row to a 2*S* double-row structure and eventually back to the single-row (at $V_R = 0.5$). Increasing V_R further resulted in the loss of lock-on over the range of negative phase angles and a transition from the 2*S* to *P*+*S* mode for the in-phase case. There was transition back to the 2*S* wake mode with a further decrease in Φ. For higher V_R the range of desynchronization increased. In the second and third parts of this paper it is shown that the occurrence of unlocked wake flow as the phase angle is varied is greater when the frequency ratio between the imposed oscillatory motions and the natural vortex shedding frequency F_{RN} is higher than unity. The vortices are synchronized in the near-wake at F_{RN} values less than unity and unlocked when $F_{RN} > 1.0$. In particular, the near-wake structures have also been shown to be synchronized for $F_R = 0.5$ and unlocked for $F_R = 2.0$.

1. Introduction

For many years there has been considerable interest in flow over an oscillating circular cylinder, due to the symmetry of the cylinder geometry combined with obvious industrial applications. These studies can be divided into three main categories depending on the motion of the cylinder: the cylinder oscillates translationally, possibly at an angle with respect

* Corresponding author. Tel.: +61399054913; fax: +61399053558.
E-mail address: john.sheridan@monash.edu (J. Sheridan).

0889-9746/$ - see front matter © 2011 Elsevier Ltd. All rights reserved.
doi:10.1016/j.jfluidstructs.2011.05.005

to the free-stream; the cylinder undergoes rotational oscillation about its axis in a mean flow; or the cylinder moves with combined oscillatory translational *and* rotational motion in either a quiescent fluid or free-stream flow. Many researchers, such as Bishop and Hassan (1964), Koopmann (1967), Bearman and Currie (1979), Sarpkaya and Isaacson (1981), Bearman et al. (1981), Bearman (1984), Williamson (1985), Williamson and Roshko (1988), Smith and Stansby (1991), Carberry et al. (2001), Carberry et al. (2005), Uzunoğlu et al. (2001), Leontini et al. (2006a), Morse and Williamson (2009) and many more have shown that the wake flow can be dramatically altered for the cylinder undergoing either in-line or transverse oscillation in a fluid stream. There has also been considerable research on the purely rotational oscillation case (see for example: Filler et al., 1991; Lo Jacono et al., 2010; Schmidt and Smith, 2004; Thiria et al., 2006; Tokumaru and Dimotakis, 1991; Wu et al., 1989). The last of the categories is a class of flow that until now has not received as much attention as the other two. Blackburn et al. (1999) found that a circular cylinder undergoing combined oscillation in a quiescent fluid has the capability to generate thrust, christened the "*swimming cylinder*". Nazarinia et al. (2009a, 2009b) extended that study and for the first time experimentally measured the flow around a circular cylinder undergoing combined translational and rotational oscillation, in both a free-stream flow and quiescent fluid, respectively. Placing the circular cylinder which is undergoing combined oscillatory motion in a free-stream has been shown to generate intriguing wake modes and has also been found by Al-Mdallal (2004), Kocabiyik and Al-Mdallal (2005) and Nazarinia et al. (2009a) to have the potential to reduce synchronization of the cylinder motion in the near-wake. Nazarinia et al. (2009a) experimentally and numerically studied the flow behind a cylinder undergoing forced combined oscillatory motion. The focus of that paper was on the effect of the phase angle (Φ) between the two motions but the influence of neither the velocity ratio nor the frequency ratio was considered. The results presented there showed that there is an unexpected loss of synchronization of the wake for a finite range of phase differences. The primary focus of the reported study here is to understand and investigate the effect of V_R and F_R on the synchronization of the cylinder motion in the near-wake. Improving our understanding of how to effect desynchronization increases the likelihood that such approaches can be used in the active or passive control of vortex-induced vibration.

2. Problem definition

Eqs. (1) and (2) define the harmonic motions of the cylinder, translationally and rotationally. It is seen from the equations that adding the rotational oscillation to the translational motion adds three more independent variables to the problem: these are the rotational amplitude, frequency and the phase angle difference between the two oscillatory motions. These are in addition to the translational amplitude and frequency, and the free-stream velocity, i.e., the Reynolds number (Eq. (5)). This results in the six dimensionless variables given below, which combine to determine the state of the flow at any time.

The forced motion of the cylinder is specified by

$$y(t) = A_t \sin(2\pi f_t t), \tag{1}$$

$$\theta(t) = A_\theta \sin(2\pi f_\theta t + \Phi). \tag{2}$$

As indicated above the six dimensionless parameters governing the flow are defined as follows:

- The translational and rotational Keulegan–Carpenter numbers (A_θ in radian):

$$\mathrm{KC}_t = \frac{U_{\max_t}}{f_t D} = \frac{2\pi A_t}{D}, \quad \mathrm{KC}_\theta = \frac{U_{\max_\theta}}{f_\theta D} = \pi A_\theta. \tag{3}$$

- The translational and rotational frequency ratios:

$$F_{Rt} = \frac{f_t}{f_N}, \quad F_{R\theta} = \frac{f_\theta}{f_N}. \tag{4}$$

- The phase angle between translation and rotation motions: Φ.
- The Reynolds number:

$$\mathrm{Re} = \frac{U_\infty D}{\nu}. \tag{5}$$

These dimensionless parameters can be combined to give two more useful parameters. These are the cylinder's velocity ratio between the translational and rotational motions, expressed as

$$V_R = \frac{U_{\max_t}}{U_{\max_\theta}} = \frac{\beta_t}{\beta_\theta}\frac{\mathrm{KC}_t}{\mathrm{KC}_\theta}, \tag{6}$$

and the frequency ratio between the translational and rotational motions, expressed as

$$F_R = \frac{f_t}{f_\theta}. \tag{7}$$

Please cite this article as: Nazarinia, M., et al., Flow over a cylinder subjected to combined translational and rotational oscillations. Journal of Fluids and Structures (2011), doi:10.1016/j.jfluidstructs.2011.05.005

Fig. 1 shows a schematic of the problem studied emphasizing the relevant features. The non-inertial Cartesian coordinate system used is defined such that the origin is located at the center of the circular cylinder (at $t=0$) with x, y, and z representing the streamwise, transverse, and spanwise directions, respectively.

3. Experimental set up and techniques

3.1. Experimental set up

All experiments were conducted in the FLAIR free-surface closed-loop water channel at the Department of Mechanical and Aerospace Engineering, Monash University. Detailed information of the set up can be found in Nazarinia et al. (2009a, 2009b), and further references therein. The cylinder used was 800 mm in length with an outer diameter of 20 mm, giving an aspect ratio of 40. The experiments were performed for a fixed average upstream velocity $U_\infty = 0.0606$ m/s giving $\mathrm{Re}_{\mathrm{avg}} = 1322$. The frequencies of the motions are fixed close to that of the natural (von Kármán) frequency ($T^{-1} = f_t = f_\theta = 0.6\ \mathrm{s}^{-1} \approx f_N$). The natural frequency was found to be equal to $f_N \approx 0.6154\ \mathrm{s}^{-1}$. The Strouhal number based on this frequency is $\mathrm{St} = f_N D/U_\infty \approx 0.203$ and the Strouhal number of the forcing is $\mathrm{St}_t \approx f_t D/U_\infty = 0.198$. The results of experiments presented here are for (a) a fixed amplitude of rotational oscillation of 1 rad and a range of $0.25 \le V_R \le 1.5$ and (b) Case 5 (see Table 1) has a reduced amplitude of rotational oscillation of 0.5 rad and $V_R = 1$. For each V_R case the phase difference angle was varied during measurements. Table 1 summarizes the data points covered in the present study.

The cylinder was oscillated translationally and rotationally using two high-resolution stepper motors. The translational stepper motor actuated a rodless in-line mounting actuator and the rotational stepper motor was connected directly to the vertically mounted cylinder. The stepper motors were controlled using a two-axis indexer and two high-resolution drivers (running at 50 800 steps rev^{-1}). Pure sinusoidal motion, as indicated in Eqs. (1) and (2), is used throughout the paper. A TTL-signal triggered other devices (camera and laser), thus images could be captured at pre-selected phase angles in the oscillation cycle (phase-locked).

3.2. Experimental techniques

The method used here to characterize the wake of this forced cylinder flow is via particle image velocimetry (PIV). PIV as a technique provides instantaneous velocity vectors of a fluid in a region of interest of the flow illuminated by a sheet of laser light. The method determines particle displacement (Δx, Δy) in a flow over a known time, Δt, and gives quantitative and non-intrusive flow measurements with high spatial resolution. In these experiments the flow fields around the sinusoidally oscillating circular cylinder were measured using PIV.

The PIV set up was based on that originally described by Adrian (1991) and further developed by, for example, Westerweel (1997). The in-house system used here was based on these approaches and developed over the past decade by Fouras et al. (2008). The flow was seeded with spherical granular polyamide particles having a mean diameter of 55 μm

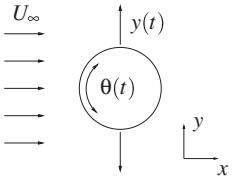

Fig. 1. Geometry of the problem studied along with the parameters relevant to the combined forced oscillations. Note that x is the streamwise direction.

Table 1
Summary of the values of A_t and A_θ used.

Case	A_t	A_θ (rad)	V_R	$U_{\max_t}$ (mm s^{-1})	$U_{\max_t}/U_\infty$	F_{RN}	F_R
1	$D/8$	1.0	0.25	9.4	0.16	1.0	1.0
2	$D/4$	1.0	0.5	18.8	0.31	1.0	1.0
3	$D/2$	1.0	1.0	37.7	0.62	1.0	1.0
4	$3D/4$	1.0	1.5	56.5	0.93	1.0	1.0
5	$D/4$	0.5	1.0	18.8	0.31	1.0	1.0
6	$D/4$	0.5	1.0	18.8	0.31	0.85–1.15	1.0
7	$D/2$	1.0	1.0	37.7	0.62	1.0	0.5
8	$D/2$	1.0	1.0	37.7	0.62	1.0	2.0

Please cite this article as: Nazarinia, M., et al., Flow over a cylinder subjected to combined translational and rotational oscillations. Journal of Fluids and Structures (2011), doi:10.1016/j.jfluidstructs.2011.05.005

and a specific gravity of 1.016. The particles were illuminated using two mini-YAG laser sources (Continuum Minilite II Q-Switched). The plane of interest for these experiments was orthogonal to the cylinder's axis (*xy*-plane) and downstream (*x*-direction) of the cylinder. A small section of the cylinder is replaced by a thin-walled transparent cylinder, whose interior is filled with distilled water to minimize refraction effects. It is located at about 9*D* from the end of cylinder. The measured *xy*-plane is located through the center of this window. The thickness of the laser sheet was measured to be a maximum of 2 mm. Pairs of images were captured on a high-resolution CCD camera with a maximum resolution of 4008×2672 pixels. The camera was equipped with a 105 mm lens (Nikon Corporation, Japan). At a particular phase of the oscillation cycle, a number of image pairs over successive cycles were taken and stored for further processing. The timing of the laser and camera triggering was controlled by a special in-house designed timing unit, with an estimated accuracy of 1 μs.

Each image pair was processed using the in-house PIV software of Fouras et al. (2008). This software uses a double-frame, cross-correlation multi-window algorithm to extract a grid of displacement vectors from the PIV images. An interrogation window of 32×32 (with an initial window size of 64×64) pixels was found to give satisfactory results with 50% overlap. More than 98% of the vectors were found to be valid for all the experiments. It was possible to obtain a measurement resolution of 127×127 vectors in each field of view. The overall field of view was 4008×2672 pixels ($6.0D \times 6.0D$).

The accuracy of our PIV set up and technique has been validated against the previous numerical and experimental results from Dütsch et al. (1998) and Tatsuno and Bearman (1990) for the *xy*- and *yz*-plane measurements. The validation case studied is for a purely translational oscillation in a quiescent fluid. Further information can be found in Nazarinia et al. (2009b).

4. Results and discussion

4.1. Effect of varying V_R

In this section the results are presented for velocity ratios of 0.25, 0.5, 1.0 and 1.5. The wake profiles around the cylinder in the streamwise direction *xy*-plane for $F_R = 1.0$ and $\mathrm{Re}_{avg} = 1322$ are investigated. It should be noted that the field-of-view does not allow us to see the flow structures that occur farther downstream, however the near-wake flow structures are the main focus of this study. For every value of V_R studied, the effect of a change of phase difference angle on the synchronization of the near-wake has also been examined. However, in this paper only selected phases are discussed and presented.

Fig. 2 presents the near-wake motion phase-locked vorticity and root-mean-square (rms) vorticity contours taken at $t=T$ for various V_R values at $\Phi = 0^\circ$, i.e., in-phase. The image at the top left of Fig. 2 shows the case where the velocity ratio is 0.25. In this case we observe a 2*S* mode (2 single vortices of opposite sign shed per period) in a single-row aligned in the medial plane but with a slight offset from the centreline. The field-of-view does not allow us to see the double-row that should occur farther downstream, as shown for example by Lamb (1932); Cimbala et al. (1988) and Johnson et al. (2004).

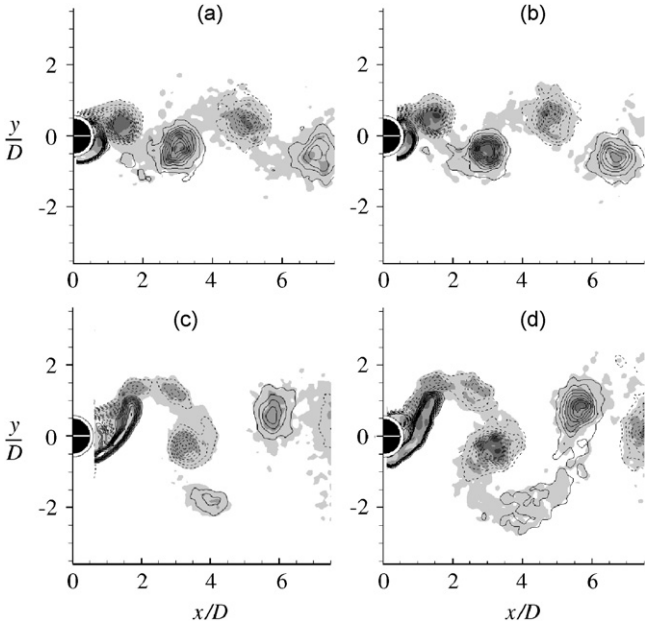

Fig. 2. Motion phase-locked vorticity contours (lines) and rms vorticity (gray-scale) contours taken at the motion-phase of $t=T$ for $A_\theta = 1.0$, $\Phi = 0^\circ$, $f_N = 0.6$ Hz, $F_R = 1$ and $\mathrm{Re}_{avg} = 1322$. The near-wake vorticity is shown for different V_R values. The flow direction is from left to right. Root-mean-square vorticity contours are evenly spaced over the range [0.02:0.1]; with $\Delta\omega_z = 0.02$, and vorticity contours are evenly spaced over the range $[-0.1{:}0.1]$; with $\Delta\omega_z rms = 0.01$: (a) V_R=0.25, (b) V_R=0.5, (c) V_R=1.0 and (d) V_R=1.5.

Please cite this article as: Nazarinia, M., et al., Flow over a cylinder subjected to combined translational and rotational oscillations. Journal of Fluids and Structures (2011), doi:10.1016/j.jfluidstructs.2011.05.005

The classification of the different vortex modes is given by Williamson and Roshko (1988). Throughout the observations it can be seen that the near-wake vortices remain coherent in the near-wake and are synchronized with the translational motion, at least up to 6D downstream. This synchronization is characterized by the repeatable pattern of the vortex shedding. Examination of the U/U_∞ and V/U_∞ velocity contours, not shown here, also suggests that the velocity structures are not changed significantly by changing the phase difference angle and that the vortices are synchronized with the translational motion, i.e., locked. Note that setting V_R to such a small value means that the rotational oscillatory speed is much higher than the translational speed. This enhanced locking-on can be explained by the rotational oscillation strongly controlling vortex shedding into the wake.

Fig. 2(b) shows the phase-locked vorticity and rms vorticity contours for V_R=0.5. In this case the vortices are still shed in a 2S single-row mode and are coherent. However, the vortices are arranged closer to each other and are less well-aligned with the medial plane, perhaps suggesting an earlier double-row transition. The rms vorticity, Fig. 2(b), along with U/U_∞ and V/U_∞ velocity contours not shown here, have a similar trend and configuration to the previously discussed case, confirming that the near-wake still synchronizes with the combined motion. However, a change in the phase difference between the two motions results in a change of shedding mode from a single-row to double-row.

Increasing V_R further to 1.0, as seen in Fig. 2(c), changes the vortex shedding mode to the signature of a $P+S$ mode (a single vortex and a vortex pair formed per cycle) in the near-wake, in comparison with the 2S mode observed in the previous cases. For this case, the vortices are shed widely apart (nearly 4D), which is readily explained by the rotational oscillation adding momentum to the translational motion. The resulting strain favors a transition to the $P+S$ wake as observed by Leontini et al. (2006b) and discussed by Nazarinia et al. (2009a).

Fig. 2(d) shows the phase-locked vorticity and rms vorticity contours for $V_R = 1.5$. The shedding mode for this case is $P+S$. The vortices are more defined in the vortex street and are observed to be synchronized with the oscillating motions. The vortices are more widely aligned than those seen in Fig. 2(c), hence forming a wider wake. This can be explained by having a faster translational peak velocity than rotational for this case.

In the results presented to this point the change of V_R was investigated by varying A_t and keeping $A_\theta = 1$ rad. In Fig. 3, A_θ was reduced to 0.5 rad while V_R was set to 1.0. This allows us to directly compare the vorticity patterns with those of Fig. 2(c), which has the same V_R but different A_θ (=1 rad). It can be observed that the vortices in Fig. 3 are all larger in size than those shown in Fig. 2 and are well-formed. The near-wakes for all of the Φ values, as can be seen in Fig. 3, are synchronized with the motions and the shedding mode is 2S. It can be seen that even though V_R (=1.0) is the same for the two cases 3 and 5 of Table 1 the near-wake structure is completely different. No transition between different shedding modes occurs as Φ is varied. In case 5, because the rotational amplitude is smaller than that of case 3, momentum is added more compactly into the flow, hence the vortices are more compact and the phase difference neither influences the synchronization of the near-wake nor the vortex shedding mode. Both rms vorticity and velocity contours confirm the

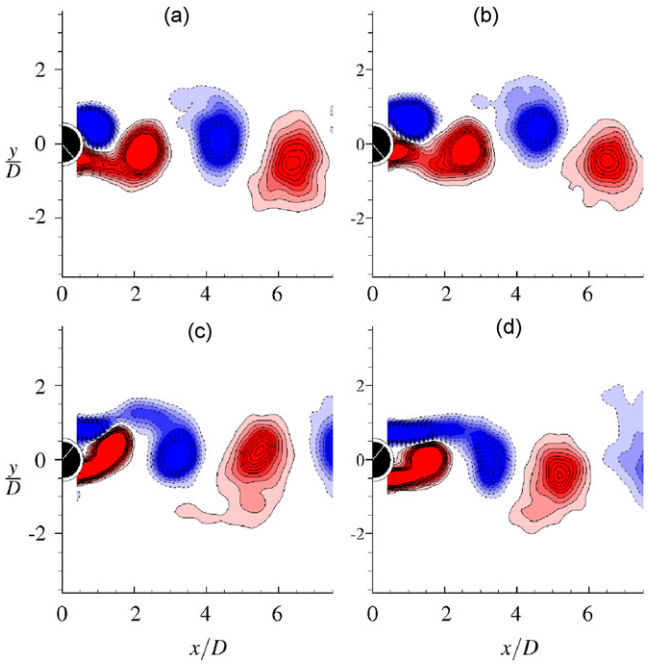

Fig. 3. Motion phase-locked vorticity contours taken at the motion-phase of $t=T$ for $f_N = 0.6$ Hz, $F_R = 1$, $A_t = D/4$, $A_\theta = 0.5$ radian and $\mathrm{Re}_{avg} = 1322$. The near-wake vorticity is shown for different Φ values. The flow direction is from left to right. Vorticity contours are evenly spaced over the range [−0.1:0.1]; with $\Delta\omega_z rms = 0.01$: (a) $\Phi = -120^\circ$, (b) $\Phi = -60^\circ$, (c) $\Phi = 60^\circ$ and (d) $\Phi = 120^\circ$.

Please cite this article as: Nazarinia, M., et al., Flow over a cylinder subjected to combined translational and rotational oscillations. Journal of Fluids and Structures (2011), doi:10.1016/j.jfluidstructs.2011.05.005

synchronization of the near-wake. The velocity patterns are qualitatively similar to the locked previous cases and no evidence of transition between states can be observed.

Figs. 4 and 5 show the near-wake motion phase-locked vorticity, rms vorticity and V/U_∞ velocity contours, respectively, taken at $t=T$ for various V_R values at $A_\theta = 1$ and $\Phi = -90^\circ$. The near-wake vortex structures and vortex modes in Fig. 4(a) and (b) are

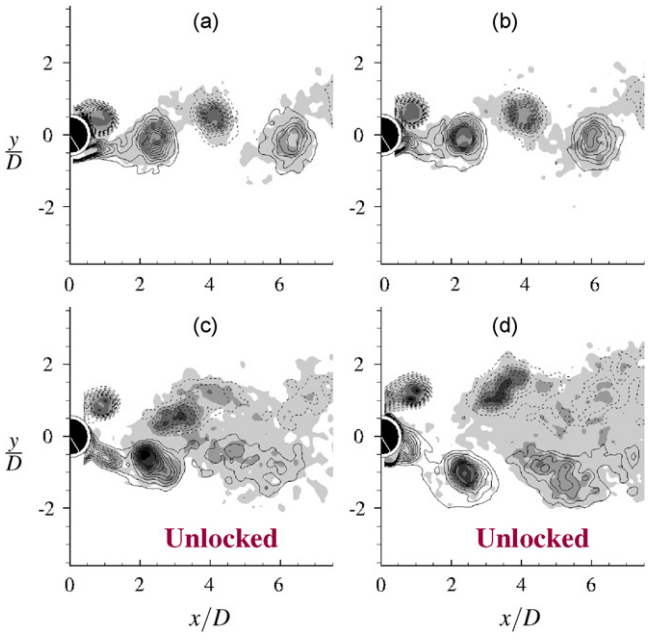

Fig. 4. Motion phase-locked vorticity contours (lines) and root-mean-square vorticity (gray-scale) contours taken at the motion-phase of $t=T$ for $A_\theta = 1.0$, $\Phi = -90^\circ$, $f_N = 0.6$ Hz, $F_R = 1$ and $\mathrm{Re}_{avg} = 1322$. The near-wake vorticity is shown for different V_R values. Of particular interest is the unlocked (asynchronous) wake with the imposed translational motion for the velocity ratios of 1.0 and 1.5. The flow direction is from left to right. Root-mean-square vorticity contours are evenly spaced for the range [0.02:0.1]; with $\Delta\omega_z = 0.02$, and vorticity contours are evenly spaced over the range $[-0.1{:}0.1]$; with $\Delta\omega_z rms = 0.01$: (a) V_R=0.25, (b) V_R=0.5, (c) V_R=1.0 and (d) V_R=1.5.

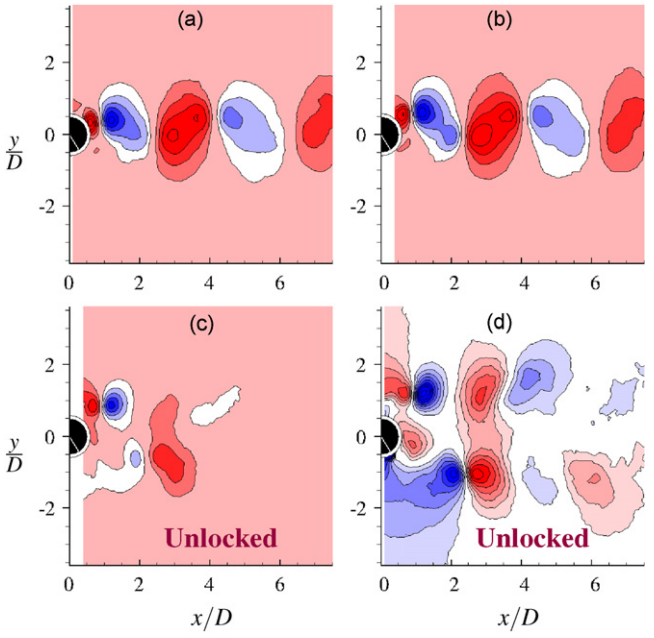

Fig. 5. Motion phase-locked V/U_∞ velocity contours taken at the motion-phase of $t=T$ for $A_\theta = 1.0$, $\Phi = -90^\circ$, $f_N = 0.6$ Hz, $F_R = 1$ and $\mathrm{Re}_{avg} = 1322$. The velocity contours are shown for different V_R values. Of particular interest is the unlocked (asynchronous) wake with the imposed translational motion for the velocity ratios of 1.0 and 1.5. The flow direction is from left to right. V/U_∞ velocity contours are evenly spaced over the range $[-0.2{:}2.4]$; with $\Delta(V/U_\infty) = 0.2$: (a) V_R=0.25, (b) V_R=0.5, (c) V_R=1.0 and (d) V_R=1.5.

Please cite this article as: Nazarinia, M., et al., Flow over a cylinder subjected to combined translational and rotational oscillations. Journal of Fluids and Structures (2011), doi:10.1016/j.jfluidstructs.2011.05.005

the same as those in Fig. 2. The vortices are not separated widely apart and remain less than 1D from the centreline. The 2S mode in a single-row aligned in the medial plane with a slight offset from the centreline was observed. These trends are consistent with the above mentioned cases. Increasing the V_R value at the same Φ was found to change the synchronization effect dramatically as can be seen in Fig. 4(c) and (d). The rms vorticity contours clearly show how the near-wake has changed its structure. In contrast to the two cases shown in Fig. 4(a) and (b), these two cases were not synchronized with the motions beyond 2D downstream. The effect of this loss of synchronization can be seen in the rapid downstream dissipation of the mean vortex structures. Only the two vortices near the cylinder remain coherent. This *a priori* surprising phenomenon might be explained by the fact that the separation between the two rows of vortices is smaller and that this arrangement of vortices is not stable. Similar behavior has been found behind elliptical cylinders Johnson et al. (2004).

Comparing the rms vorticity contours and V/U_∞ of this case (Figs. 4 and 5) with the previous cases shows that there is a dramatic change of patterns in the velocity contours between the synchronized (locked) and desynchronized (unlocked) cases. The synchronized velocity patterns are all well organized and qualitatively similar to each other for the entire downstream domain shown in the images. Fig. 5 clearly shows that the V/U_∞ velocity contour pattern changes dramatically for the unlocked cases. For distances farther downstream than approximately 3D the phase-averaged locations of vortices are much less well-defined, so there is considerable variation from one cycle to the next for this part of the wake.

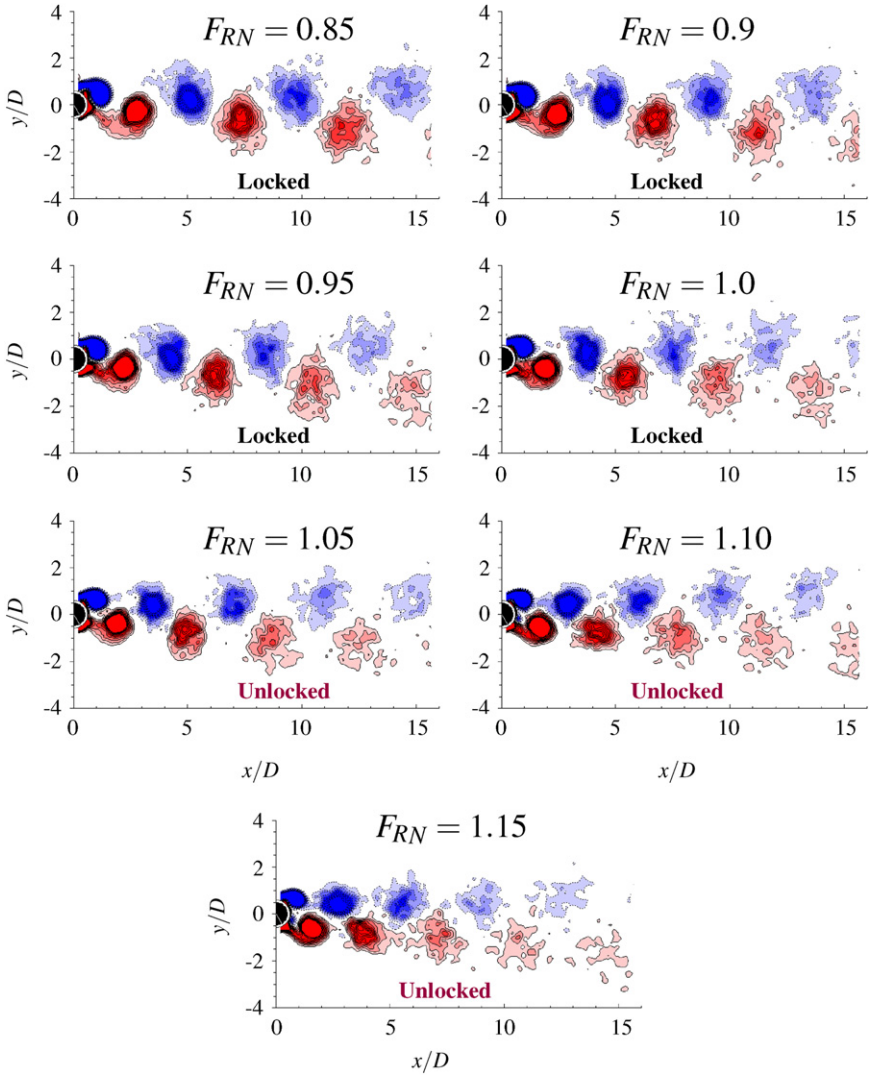

Fig. 6. Motion phase-locked vorticity contours taken at the motion-phase of $t=T$ for $A_t = D/4$, $A_\theta = 0.5$ rad, $f_N = 0.6$ Hz, $V_R = 1.0$, $\Phi = -90^\circ$ and $\mathrm{Re}_{avg} = 1322$. The near-wake vorticity is shown for different frequency ratios. Of particular interest is the asynchronous (unlocked) wake with the imposed translational motion for the frequency ratios between the oscillatory motions and the natural vortex shedding of $F_{RN} = 0.9$ to 1.15. The flow direction is from left to right. Vorticity contours are evenly spaced over the range $[-0.2{:}0.2]$; with $\Delta\omega_z = 0.02$.

Please cite this article as: Nazarinia, M., et al., Flow over a cylinder subjected to combined translational and rotational oscillations. Journal of Fluids and Structures (2011), doi:10.1016/j.jfluidstructs.2011.05.005

4.2. Effect of varying F_{RN}

Figs. 6 and 7 present near-wake motion phase-locked vorticity and V/U_∞ velocity contours, respectively, taken at $t=T$ for various F_{RN} ($=F_{Rt}=F_{R\theta}$) at $A_t=D/4$, $A_\theta=0.5$, $V_R=1.0$ and $\Phi=-90^\circ$. Nazarinia et al. (2009a) showed that the near-wake becomes unlocked at $\Phi=-90^\circ$. This occurred when the two motions were oscillating at the same frequency, i.e., $F_R=F_{RN}=1.0$. To investigate the effect of sensitivity of the synchronization of the near-wake, a series of experiments were conducted in which the frequency ratio between the imposed oscillatory motions and the natural vortex shedding frequency was varied from $F_{RN}=0.85$ to 1.15 in increments of 0.05. The top left image of Fig. 6 shows the vorticity contours for $F_{RN}=0.85$. The very near-wake vortex structures are coherent, well-defined and synchronized. As the F_{RN} ratio is increased the region where the near-wake vortices are coherent and well-defined becomes shorter and gets closer to the cylinder. It can also be seen that the structures start to dissipate in the far-wake. Increasing the F_R ratio to 0.95 and 1.0 shows that the dissipation region becomes shorter and gets closer to the near-wake region. The near-wake vortices are all still locked; this can also be seen from Fig. 7. When the frequency ratio is raised above unity the near-wake also starts to become desynchronized and by increasing the F_{RN} ratio this desynchronization region becomes smaller approaching the cylinder. This can also be clearly seen in Fig. 7, and verified by observing the dynamics of the wake as recorded in animations. The recorded animations clearly showed the lock-on behavior but this is not as evident in the figures presented here.

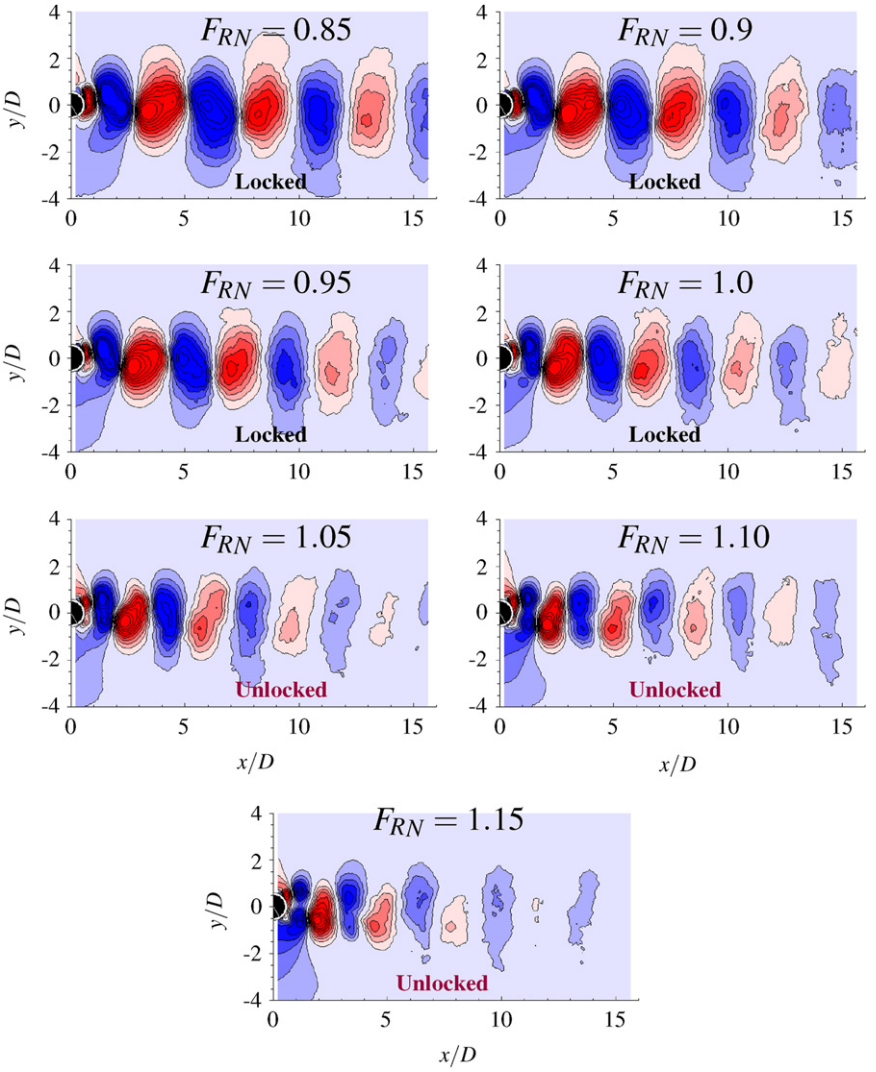

Fig. 7. Motion phase-locked V/U_∞ velocity contours taken at the motion-phase of $t=T$ for $A_t=D/4$, $A_\theta=0.5$ rad, $f_N=0.6$ Hz, $V_R=1.0$, $\Phi=-90^\circ$ and $Re_{avg}=1322$. The near-wake transverse velocity is shown for different frequency ratios. Of particular interest is the asynchronous (unlocked) wake with the imposed translational motion for the frequency ratios between the oscillatory motions and the natural vortex shedding of $F_{RN}=0.9$ to 1.15. The flow direction is from left to right. V/U_∞ velocity contours are evenly spaced over the range [0.2:7.4]; with $\Delta(V/U_\infty)=0.4$.

Please cite this article as: Nazarinia, M., et al., Flow over a cylinder subjected to combined translational and rotational oscillations. Journal of Fluids and Structures (2011), doi:10.1016/j.jfluidstructs.2011.05.005

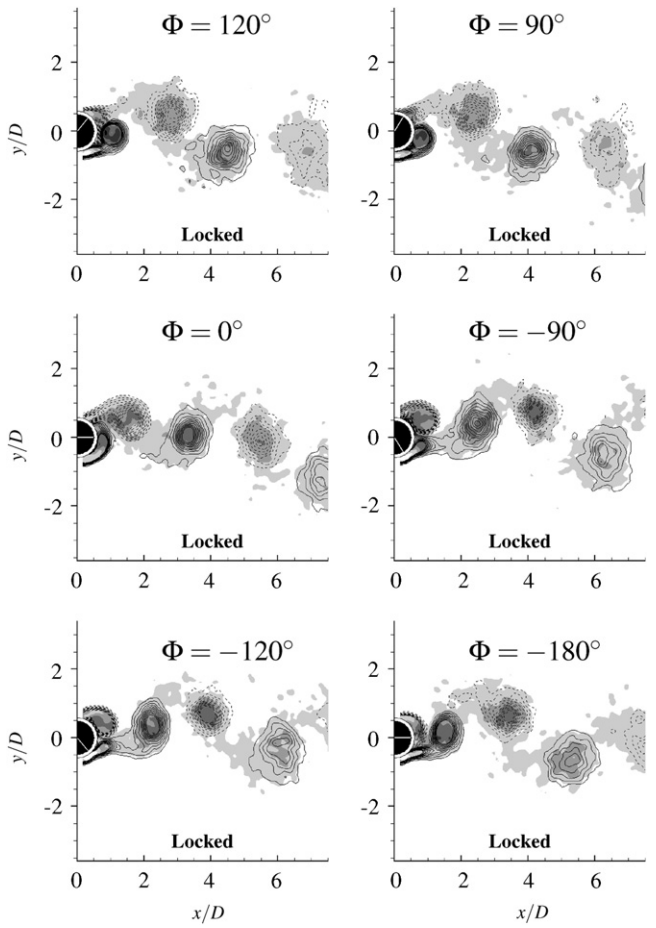

Fig. 8. Motion phase-locked vorticity contours (lines) and root-mean-square vorticity (gray-scale) contours taken at the motion-phase of $t=T$ for $A_t = D/2$, $A_\theta = 1.0$ rad, $f_N = 0.6$ Hz, $V_R = 1$, $F_R = 0.5$ and $\mathrm{Re} = 1251$. The near-wake rms vorticity is shown for different phase angle differences between the two imposed oscillatory motions. Of particular interest is the asynchronous (unlocked) wake with the imposed translational motion for the phase $\Phi = -90^\circ$, -120°, -150° and $\pm 180^\circ$. The flow direction is from left to right.

4.3. Effect of varying F_R

All the results presented in the previous sections were obtained when the frequencies of the translational and rotational oscillations were the same, i.e., $F_R = 1$. This section deals with the case where the frequencies are different. Two cases with $F_R = 0.5$ and $F_R = 2$ are presented. Fig. 8 presents near-wake motion vorticity and rms vorticity contours taken at $t=T$ for various phase angle differences at $A_t = D/2$, $A_\theta = 0.5$, $V_R = 1.0$, $F_R = 0.5$ and $\mathrm{Re}_{avg} = 1322$. The top left image of Fig. 8 shows the $\Phi = 120^\circ$ case; as seen previously, we observe a 2S mode in a single-row. Interestingly, and in contrast to all the previous cases, the vortices are not shed in the medial plane. They are shed with an angle to the centreline. Similar patterns were seen in all the cases presented at $F_R = 0.5$. It can also be seen that all the vortices are well-defined and coherent. They are also more widely separated from each other in the transverse direction. As the phase angle difference reduces the vortices approach each other and the cylinder. The angled shedding of the vortices was observed for all the phase angle differences studied. Fig. 8 clearly shows that there is no transition between modes in these cases. From Fig. 9 it can be seen that for all the different Φ cases the vortices unlocked when $F_R = 2.0$. It was observed in the experiments that only the negatively signed vortex attached to the cylinder is synchronized; however, when it is shed it cannot match to the natural shedding frequency and becomes desynchronized. As the translational motion is oscillating at a higher frequency than the rotational motion in this case the rotational motion does not add as much momentum to the shed vortices as it does for the $F_R < 1$ cases. The vortices dissipate quickly beyond 3D downstream of the cylinder and are not as well-defined and coherent as in the $F_R < 1$ cases.

5. Conclusions

In this work we have experimentally investigated the near-wake flow structures of flow past a cylinder undergoing a combined translational and rotational oscillatory motion. The effect of the velocity ratio between the two forced motions

Please cite this article as: Nazarinia, M., et al., Flow over a cylinder subjected to combined translational and rotational oscillations. Journal of Fluids and Structures (2011), doi:10.1016/j.jfluidstructs.2011.05.005

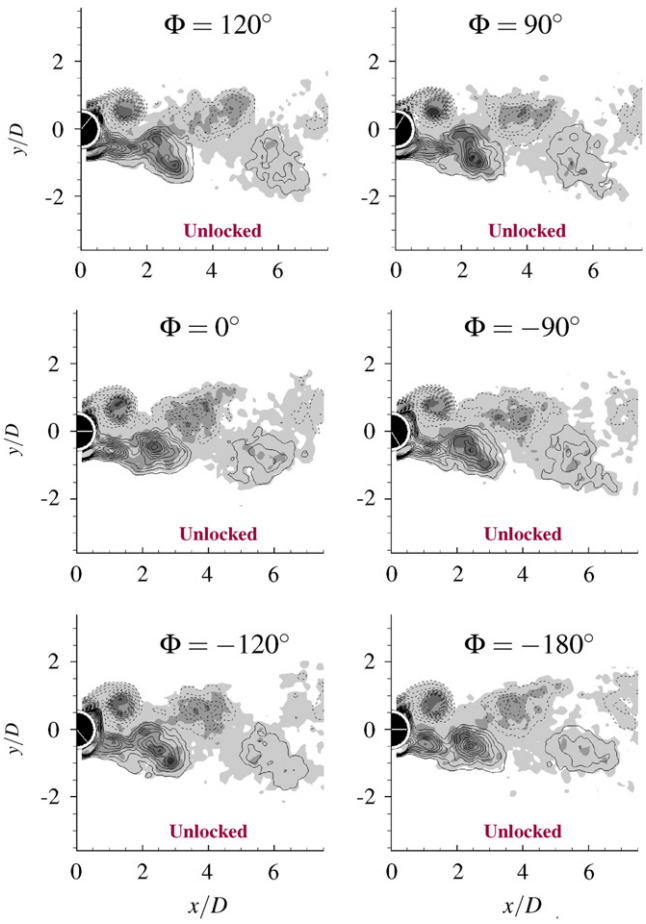

Fig. 9. Motion phase-locked vorticity contours (lines) and root-mean-square vorticity (gray-scale) contours taken at the motion-phase of $t=T$ for $A_t = D/2$, $A_\theta = 1.0$ rad, $f_N = 0.6$ Hz, $V_R = 1$, $F_R = 2$ and $\mathrm{Re} = 1251$. The near-wake rms vorticity is shown for different phase angle differences between the two imposed oscillatory motions. Of particular interest is the asynchronous (unlocked) wake with the imposed translational motion for the phase $\Phi = -90^\circ$, -120°, -150° and $\pm 180^\circ$. The flow direction is from left to right.

for a given Reynolds number and for different combinations of Φ reveals that regular vortex shedding can be suppressed for particular phase differences and V_R values. The range of phase difference for which the suppression occurs depends on V_R and F_R of the oscillations and the oscillation frequency ratio to natural vortex shedding frequency of a fixed cylinder, F_{RN}. At the lower values of V_R, over the range of phase difference angles studied, no transition to different wake modes is observed. All the vortices in the near-wake region of the cylinder are synchronized and coherently shed in the 2S mode. Increasing the V_R value beyond a certain value changes the wake modes and the synchronization of the vortices in the near-wake. The vortices become unlocked and less coherent as V_R is increased further for a range of Φ. The effect of changing translational and rotational amplitudes for a given V_R, i.e., $V_R = 1.0$, was also investigated. It appears that at higher A_t and lower A_θ the vortices in the near-wake are more compact and larger in size. The effects of frequency ratios between the two forced motions relative to the natural vortex shedding frequency and also between the two forced motions relative to themselves have also been studied. The experimental results showed that for $F_{RN} < 1.0$ and $F_R = 0.5$ the near-wake vortices are all synchronized to the oscillatory motions whereas for $F_{RN} > 1.0$ and $F_R = 2.0$ they are unlocked. This experimental study raised several interesting questions arising from the features seen to determine the wake modes in the near-wake of the combined oscillatory cylinder in free-stream. One particularly interesting question is whether the desynchronized state has a chaotic or quasi-periodic form. However, an intensive study of this would require further investigation using higher frequency sampling than is possible with our current PIV system. This could possibly be pursued, however, by a combination of Laser Doppler Anemometer experiments and numerical modeling.

Acknowledgments

MN acknowledges the support of a Monash Graduate Scholarship (MGS) and a Monash International Postgraduate Research Scholarship (MIPRS). All authors acknowledge the support from the Australian Research Council through ARC

Discovery Project Grant Number DP0774525 and through the Australian Partnership for Advanced Computing/National Computing Infrastructure (APAC/NCI) Merit Allocation Scheme.

References

Adrian, R.J., 1991. Particle-imaging techniques for experimental fluid mechanics. Annual Review of Fluid Mechanics 23, 261–304.
Al-Mdallal, Q.M., 2004. Analysis and computation of the cross-flow past an oscillating cylinder with two degrees of freedom. Ph.D. Thesis, Memorial University of Newfoundland.
Bearman, P.W., 1984. Vortex shedding from oscillating bluff bodies. Annual Review of Fluid Mechanics 16 (1), 195–222.
Bearman, P.W., Currie, I.G., 1979. Pressure fluctuation measurements on an oscillating circular cylinder. Journal of Fluid Mechanics 91, 661–677.
Bearman, P.W., Graham, J.M.R., Naylor, P., Obasaju, E.D., 1981. The role of vortices in oscillatory flow about bluff cylinders. In: International Symposium on Hydrodynamics in Ocean Engineering, Trondheim, Norway, pp. 621–635.
Bishop, R.E.D., Hassan, A.Y., 1964. The lift and drag forces on a circular cylinder oscillating in a flowing fluid. Proceedings of the Royal Society of London, Series A 277 (68) 51–75.
Blackburn, H.M., Elston, J.R., Sheridan, J., 1999. Bluff-body propulsion produced by combined rotary and translational oscillation. Physics of Fluids 11 (1), 4–6.
Carberry, J., Sheridan, J., Rockwell, D., 2001. Force and wake modes of an oscillating cylinder. Journal of Fluid and Structures 15, 523–532.
Carberry, J., Sheridan, J., Rockwell, D., 2005. Controlled oscillations of a cylinder: forces and wake modes. Journal of Fluid Mechanics 538, 31–69.
Cimbala, J.M., Nagib, H.M., Roshko, A., 1988. Large structure in the far wakes of two-dimensional bluff bodies. Journal of Fluid Mechanics 190, 265–298.
Dütsch, H., Durst, F., Becker, S., Lienhart, H., 1998. Low-Reynolds-number flow around an oscillating circular cylinder at low Keulegan–Carpenter numbers. Journal of Fluid Mechanics 360, 249–271.
Filler, J.R., Marston, P.L., Mih, W.C., 1991. Response of the shear layers separating from a circular cylinder to small amplitude rotational oscillations. Journal of Fluid Mechanics 231, 481–499.
Fouras, A., Lo Jacono, D., Hourigan, K., 2008. Target-free stereo PIV: a novel technique with inherent error estimation and improved accuracy. Experiments of Fluids 44 (2), 317–329.
Johnson, S.A., Thompson, M.C., Hourigan, K., 2004. Predicted low frequency structures in the wake of elliptical cylinders. European Journal of Mechanics B—Fluids 23, 229–239.
Kocabiyik, S., Al-Mdallal, Q.M., 2005. Bluff-body flow created by combined rotary and translational oscillation. Fluid Structure Interaction and Moving Boundary Problems, vol. 84. WIT Press, Southampton, UK, pp. 195–203.
Koopmann, G.H., 1967. The vortex wakes of vibrating cylinders at low Reynolds numbers. Journal of Fluid Mechanics 28, 501–512.
Lamb, H., 1932. Hydrodynamics. Cambridge University Press, Dover, NY.
Leontini, J.S., Stewart, B.E., Thompson, M.C., Hourigan, K., 2006a. Predicting vortex-induced vibration from driven oscillation results. Applied Mathematical Modelling 30, 1096–1102.
Leontini, J.S., Stewart, B.E., Thompson, M.C., Hourigan, K., 2006b. Wake state and energy transitions of an oscillating cylinder at low Reynolds number. Physics of Fluids 18 (3), 067101.
Lo Jacono, D., Leontini, J.S., Thompson, M.C., Sheridan, J., 2010. Modification of three-dimensional transition in the wake of a rotationally oscillating cylinder. Journal of Fluid Mechanics 643, 349–362.
Morse, T.L., Williamson, C.H.K., 2009. Fluid forcing, wake modes, and transitions for a cylinder undergoing controlled oscillations. Journal of Fluid and Structures 25 (4), 697–712.
Nazarinia, M., Lo Jacono, D., Thompson, M.C., Sheridan, J., 2009a. Flow behind a cylinder forced by a combination of oscillatory translational and rotational motions. Physics of Fluids 21 (5), 051701.
Nazarinia, M., Lo Jacono, D., Thompson, M.C., Sheridan, J., 2009b. The three-dimensional wake of a cylinder undergoing a combination of translational and rotational oscillation in a quiescent fluid. Physics of Fluids 21 (6), 064101.
Sarpkaya, T., Isaacson, M., 1981. Mechanics of Wave Forces on Offshore Structures. Van Nostrand Reinhold Company.
Schmidt, C.W., Smith, D.R., 2004. An investigation of the wake behind a circular cylinder with sinusoidal rotational forcing. In: 42nd AIAA Aerospace Science Meeting & Exhibit, Reno, NV, USA, pp. 1–9. AIAA-2004-0924.
Smith, P.A., Stansby, P.K., 1991. Viscous oscillatory flows around cylindrical bodies at low Keulegan–Carpenter numbers using the vortex method. Journal of Fluid and Structures 5, 339–361.
Tatsuno, M., Bearman, P.W., 1990. A visual study of the flow around an oscillating circular cylinder at low Keulegan–Carpenter numbers and low Stokes numbers. Journal of Fluid Mechanics 211, 157–182.
Thiria, B., Goujon-Durand, S., Wesfreid, J.E., 2006. The wake of a cylinder performing rotary oscillations. Journal of Fluid Mechanics 560, 123–147.
Tokumaru, P.T., Dimotakis, P.E., 1991. Rotary oscillation control of a cylinder wake. Journal of Fluid Mechanics 224, 77–90.
Uzunoğlu, B., Tan, M., Price, W.G., 2001. Low-Reynolds-number flow around an oscillating cylinder using a cell viscous boundary element method. Int. Journal of Numerical Methods in Engineering. 50, 2317–2338.
Westerweel, J., 1997. Fundamentals of digital particle image velocimetry. Meas. Sci. Technol. 8, 1379–1392.
Williamson, C.H.K., 1985. Sinusoidal flow relative to circular cylinders. Journal of Fluid Mechanics 155, 141–174.
Williamson, C.H.K., Roshko, A., 1988. Vortex formation in the wake of an oscillating cylinder. Journal of Fluids and Structures 2 (4), 355–381.
Wu, J.M., Mo, J.D., Vakili, A.D., 1989. On the wake of a cylinder with rotational oscillations. In: AIAA 2nd Shear Flow Conference, pp. 1–10. AIAA-89-1024.

Please cite this article as: Nazarinia, M., et al., Flow over a cylinder subjected to combined translational and rotational oscillations. Journal of Fluids and Structures (2011), doi:10.1016/j.jfluidstructs.2011.05.005